

# Local density of states of a quarter-filled one-dimensional Mott insulator with a boundary

Dirk Schuricht<sup>1,2</sup>

<sup>1</sup>*Institute for Theory of Statistical Physics, RWTH Aachen, 52056 Aachen, Germany*

<sup>2</sup>*JARA-Fundamentals of Future Information Technology*

(Dated: July 7, 2018)

We study the low-energy limit of a quarter-filled one-dimensional Mott insulator. We analytically determine the local density of states in the presence of a strong impurity potential, which is modeled by a boundary. To this end we calculate the Green function using field theoretical methods. The Fourier transform of the local density of states shows signatures of a pinning of the spin-density wave at the impurity as well as several dispersing features at frequencies above the charge gap. These features can be interpreted as propagating spin and charge degrees of freedom. Their relative strength can be attributed to the “quasi-fermionic” behavior of charge excitations with equal momenta. Furthermore, we discuss the effect of bound states localized at the impurity. Finally, we give an overview of the local density of states in various one-dimensional systems and discuss implications for scanning tunneling microscopy experiments.

PACS numbers: 68.37.Ef, 71.10.Pm, 72.80.Sk

## I. INTRODUCTION

Over the past decades scanning tunneling microscopy (STM) and spectroscopy techniques have been established as an important experimental tool to study strongly correlated electron systems with a spatial resolution down to the atomic scale. In these experiments the tunneling current between the sample and the STM tip is measured as a function of its position and the applied voltage. The tunneling current is directly related<sup>1</sup> to the local density of states (LDOS) in the sample; thus STM experiments provide a tool to investigate the spatial dependence of the LDOS, which may arise for example due to impurities. These spatial modulations can be analyzed in terms of the Fourier transform of the tunneling conductance which is directly proportional to the Fourier transform of the LDOS. Using this method of analyzing STM data one can infer informations about the bulk state of matter like the properties of its quasi-particle excitations. For example, this has been used to study high-temperature superconductors<sup>2</sup> as well as carbon nanotubes<sup>3</sup>.

Theoretical studies of the LDOS and STM in the presence of boundaries have been carried out in particular for one-dimensional systems including Luttinger liquids<sup>4–8</sup>, open Hubbard chains<sup>5,9</sup>, and charge-density wave (CDW) states<sup>10,11</sup>. In these systems the coupling to impurities is relevant<sup>11–13</sup>, which leads, at sufficiently low energies, to an effective cutting of the system into disconnected pieces. In this sense the effect of an impurity can be modeled by a boundary condition. Previous studies of the Fourier transform of the LDOS in both gapless<sup>6–8</sup> and gapped<sup>10,11</sup> systems revealed a pinning of the CDW at the impurity as well as individually propagating spin and charge degrees of freedom.

Here we study a quarter-filled one-dimensional Mott insulator in the presence of a strong impurity poten-

tial. It has been established<sup>13,14</sup> that for sufficiently strong interactions double Umklapp processes are relevant and generate a gap in the charge sector. As a microscopic realization one may think of a quarter-filled Hubbard model extended by including nearest-neighbor interactions, which possesses<sup>15</sup> an insulating phase for sufficiently strong repulsions. Experimentally these systems are relevant for the description of organic quasi-one-dimensional conductors, i.e. the Bechgaard and Fabre salts<sup>16</sup>.

In this article we study the low-energy behavior of the LDOS by employing the field theoretical description of the Mott insulator. The spectrum consists of massless spin excitations (spinons) carrying spin  $\pm 1/2$  but no charge and massive charge excitations (solitons and antisolitons) carrying charge  $\pm e/2$  but no spin. In this framework the impurity is modeled by a boundary for the collective excitations. In particular, we will focus on signatures of dispersing quasiparticles in the spatial Fourier transform of the LDOS, as they have been clearly observed in similar studies of Luttinger liquids<sup>6–8</sup> and half-filled Mott insulators as well as CDW states<sup>10,11</sup>. The spectral function of the translationally invariant, quarter-filled Mott insulator has been previously derived<sup>17</sup> by Essler and Tsvelik. From the quantum numbers stated above it is clear that an electron will fractionalize into at least one spinon and two antisolitons. Thus the spectral function exhibits a featureless scattering continuum of at least three excitations, which is also consistent with experimental results<sup>18</sup> from angle-resolved photoelectron spectroscopy on Bechgaard salts.

This article is organized as follows. In Sec. II we will briefly discuss the field theoretical description of the quarter-filled Mott insulator. In Sec. III we present our results for the single-particle Green function. This will then be used to derive an analytic expression for the LDOS, which we will discuss in detail in Sec. IV. Our main result is presented in Eq. (15) as well as Figs. 1

and 2, which show the Fourier transform of the LDOS in the presence of an impurity. Surprisingly, we find two dispersing features which follow the dispersion relations (19) and (20) respectively. These features can be interpreted as arising from an antisoliton or a spinon-antisoliton pair propagating between the position of the STM tip and the impurity. In addition, we observe a non-dispersing singularity at momentum  $Q = 2k_F$  which is indicative of a pinning of a spin-density wave (SDW) at the boundary. A detailed analysis further reveals dispersing features originating in propagating spinons and antisoliton pairs. The suppression of these features is attributed to the “quasi-fermionic” behavior of antisolitons with equal momenta. Finally we explain the different findings in the spectral function and the LDOS. In Sec. V we discuss the effect of possible boundary bound states on the LDOS and in Sec. VI we compare our results to the half-filled Mott insulator studied<sup>10,11</sup> previously. Finally, in Sec. VII we set our results in the context of other one-dimensional systems and discuss implications for STM experiments on quasi-one-dimensional materials. Readers mainly interested in the qualitative features of the LDOS may start with this section and study the detailed results afterwards. Technical details have been moved to the appendix.

## II. THE MODEL

As the underlying microscopic model for the quarter-filled Mott insulator one may start with the extended Hubbard model<sup>13</sup>

$$H_{\text{Hubbard}} = -t \sum_{j,\sigma} \left[ c_{j,\sigma}^\dagger c_{j+1,\sigma} + c_{j+1,\sigma}^\dagger c_{j,\sigma} \right] + U \sum_j n_{j,\uparrow} n_{j,\downarrow} + V \sum_j n_j n_{j+1}, \quad (1)$$

where  $c_{j,\sigma}^\dagger$  and  $c_{j,\sigma}$  are electron creation and annihilation operators at site  $j$  with spin  $\sigma = \uparrow, \downarrow$ ,  $n_{j,\sigma} = c_{j,\sigma}^\dagger c_{j,\sigma}$ , and  $n_j = n_{j,\uparrow} + n_{j,\downarrow}$ . At quarter filling and for sufficiently large on-site and nearest-neighbor repulsions  $U, V \geq 4t$  this model possesses a Mott insulating phase<sup>15</sup> which can be thought of as a microscopic realization of the field-theoretical system we will study below. The extended Hubbard model (1) can be used as an effective model for the description of Bechgaard salts<sup>16</sup>; its spectral and transport properties have been investigated in detail using various techniques<sup>13,19</sup>.

Instead of working with the microscopic model (1) we will study here the corresponding low-energy field theory. The continuum description is obtained by focusing on the degrees of freedom around the Fermi points  $\pm k_F$ . We introduce slowly varying right- and left-moving Fermi fields as

$$\frac{c_{j,\sigma}}{\sqrt{a_0}} \rightarrow \Psi_\sigma(x) = e^{ik_F x} R_\sigma(x) + e^{-ik_F x} L_\sigma(x), \quad (2)$$

and similarly for the electron creation operators. Here  $a_0$  denotes the lattice spacing,  $x = ja_0$ , and the Fermi momentum is given by  $k_F = \pi/4a_0$  at quarter filling. The impurity potential is assumed to be strong such that we can model it by a boundary condition on the continuum electron field

$$\Psi_\sigma(x=0) = 0. \quad (3)$$

Using standard bosonization of the right- and left-moving Fermi fields it was shown<sup>13,14</sup> that double Umklapp processes result in a cosine term in the charge sector, which is relevant at low energies and generates a gap. Thus the effective low-energy Hamiltonian is given by<sup>20</sup>

$$H = H_c + H_s, \quad (4)$$

$$H_c = \frac{v_c}{16\pi} \int_{-\infty}^0 dx \left[ (\partial_x \Phi_c)^2 + (\partial_x \Theta_c)^2 \right] - \frac{g_c}{(2\pi)^2} \int_{-\infty}^0 dx \cos(\beta \Phi_c), \quad (5)$$

$$H_s = \frac{v_s}{16\pi} \int_{-\infty}^0 dx \left[ (\partial_x \Phi_s)^2 + (\partial_x \Theta_s)^2 \right], \quad (6)$$

where, as a consequence of (3), the canonical Bose fields  $\Phi_{c,s}$  are subject to the hard-wall boundary conditions

$$\Phi_{c,s}(x=0) = 0. \quad (7)$$

The fields  $\Theta_{c,s}$  are dual to  $\Phi_{c,s}$ . The charge and spin velocities  $v_{c,s}$ , the Luttinger parameter  $\beta$ , and the coupling constant  $g_c$  are functions of the hopping and interactions in an underlying microscopic model. Within the field theory they can be viewed as phenomenological parameters. Experimental estimates<sup>21</sup> for the Luttinger parameter in the Bechgaard salts yield  $\beta^2 \approx 0.9$ .

In the bosonization procedure leading to the effective low-energy Hamiltonian (4) the explicit relation between the Fermi and the Bose fields is given by<sup>17,22</sup>

$$R_\sigma^\dagger = \frac{\eta_\sigma}{\sqrt{2\pi}} \exp \left[ \frac{i}{4} \left( \frac{\beta}{2} \Phi_c + \frac{2}{\beta} \Theta_c \right) \right] \times \exp \left[ \frac{i}{4} f_\sigma (\Phi_s + \Theta_s) \right], \quad (8)$$

$$L_\sigma^\dagger = \frac{\eta_\sigma}{\sqrt{2\pi}} \exp \left[ -\frac{i}{4} \left( \frac{\beta}{2} \Phi_c - \frac{2}{\beta} \Theta_c \right) \right] \times \exp \left[ -\frac{i}{4} f_\sigma (\Phi_s - \Theta_s) \right], \quad (9)$$

where the Klein factors  $\eta_\sigma$  satisfy the anticommutation relations  $\{\eta_\sigma, \eta_{\sigma'}\} = 2\delta_{\sigma\sigma'}$  and  $f_\uparrow = 1 = -f_\downarrow$ .

The charge excitations are described by the sine-Gordon model on the half-line (5). For  $\beta < 1$  the cosine term is relevant and generates a gap. The excitations are massive solitons and antisolitons which carry charges  $\pm e/2$  respectively. They possess a relativistic dispersion relation; we parametrize their energy and momentum in the usual way using the rapidity  $\theta$  by

$$E = \Delta \cosh \theta, \quad P = \frac{\Delta}{v_c} \sinh \theta. \quad (10)$$

The soliton mass  $\Delta$  is a function<sup>23</sup> of the bare parameters  $g_c$  and  $\beta$  but will be viewed here as a phenomenological parameter replacing the coupling constant  $g_c$ . In the regime  $1/2 \leq \beta^2$  solitons and antisolitons are the only excitations in the charge sector; for  $\beta^2 < 1/2$  propagating breather (soliton-antisoliton) bound states exist as well. At the Luther-Emery point (LEP)  $\beta^2 = 1/2$  the charge sector is equivalent to a free massive Dirac theory<sup>24</sup>. The sine-Gordon model (5) with the boundary condition (7) is integrable<sup>25,26</sup>, which we will use below to calculate the necessary correlation functions of right- and left-moving Fermi fields. The spin sector (6) describes massless relativistic spinon excitations which propagate with velocity  $v_s$  and carry spin  $\pm 1/2$ . We have already assumed spin rotational invariance, i.e. a possible Luttinger parameter in the spin sector is set to one.

We note that the half-filled Mott insulator studied previously<sup>10,11</sup> possesses the same effective low-energy Hamiltonian (4)–(6). The difference to the quarter-filled case studied in this article is given<sup>22</sup> by the bosonization relations (8) and (9) for the right- and left-moving Fermi fields. This leads to differing Green functions as well as LDOS. We will proceed with the presentation of the results for the quarter-filled Mott insulator and present a detailed comparison to the half-filled system in Sec. VI.

### III. GREEN FUNCTION

In order to derive the LDOS below we calculate the time-ordered Green function in Euclidean space,

$$G_{\sigma\sigma'}(\tau, x_1, x_2) = -\langle 0_b | \mathcal{T}_\tau \Psi_\sigma(\tau, x_1) \Psi_{\sigma'}^\dagger(0, x_2) | 0_b \rangle, \quad (11)$$

where  $|0_b\rangle$  is the ground state of (4) in the presence of the boundary and  $\tau = it$  denotes imaginary time. At low energies we can linearize around the Fermi points  $\pm k_F$ , which results in

$$G_{\sigma\sigma'} = e^{ik_F(x_1-x_2)} G_{\sigma\sigma'}^{RR} + e^{-ik_F(x_1-x_2)} G_{\sigma\sigma'}^{LL} + e^{ik_F(x_1+x_2)} G_{\sigma\sigma'}^{RL} + e^{-ik_F(x_1+x_2)} G_{\sigma\sigma'}^{LR}, \quad (12)$$

where e.g.  $G_{\sigma\sigma'}^{RL} = -\langle 0_b | \mathcal{T}_\tau R_\sigma(\tau, x_1) L_{\sigma'}^\dagger(0, x_2) | 0_b \rangle$ . For the calculation of the LDOS we have to set  $x_1 = x_2$  below. In particular, we will focus on the spatial Fourier transform of the LDOS as physical properties can be more easily identified. The four terms in the decomposition (12) then contribute in different regions in momentum space, i.e.  $G_{\sigma\sigma'}^{RL}$  and  $G_{\sigma\sigma'}^{LR}$  contribute for  $Q \approx \pm 2k_F$  while  $G_{\sigma\sigma'}^{RR}$  and  $G_{\sigma\sigma'}^{LL}$  contribute for  $Q \approx 0$ . In the translationally invariant system right- and left-moving fields in the spin sector decouple which results in  $G_{\sigma\sigma'}^{RL} = G_{\sigma\sigma'}^{LR} = 0$ . The presence of a boundary couples right and left sectors and concomitantly the Fourier transform of the Green function (12) acquires a non-zero component at  $Q \approx \pm 2k_F$ . We will focus on the  $2k_F$ -part of the Green function and the LDOS in the following, since this provides a particularly clean way of investigating boundary

effects. We note that the other components of the Green function (12) can be calculated in the same way.

Due to the spin-charge separated Hamiltonian (4) the Green function  $G_{\sigma\sigma'}^{RL}$  factorizes into a product of correlation functions in the spin and charge sectors. The correlation functions in the spin sector can be straightforwardly derived using standard methods like boundary conformal field theory<sup>27</sup>. On the other hand, the integrability of the sine-Gordon model on the half-line (6) enables us to calculate correlation functions in the charge sector using the boundary state formalism<sup>25</sup> together with a form-factor expansion<sup>22,28,29</sup>. This yields the following result for the  $2k_F$ -component of the Green function

$$G_{\sigma\sigma'}^{RL}(\tau, x_1, x_2) = -\frac{1}{2\pi} \frac{\delta_{\sigma\sigma'}}{\sqrt{v_s\tau - i(x_1 + x_2)}} \sum_{k=0}^{\infty} \mathcal{G}_k(\tau, x_1, x_2). \quad (13)$$

The infinite series originates from the applied form-factor expansion, which constitutes an expansion of correlation functions in the number of contributing solitons and antisolitons. In App. A we derive explicit expressions for the first three terms  $\mathcal{G}_k$  which correspond to two-particle processes in the charge sector. We note that (13) is valid at zero temperature. The effect of small temperatures  $T \ll \Delta$  on the gapless spin sector can be incorporated using conformal field theory<sup>27</sup> as discussed for the half-filled Mott insulator in Ref. 11. In the next section we use the result (13) to derive the Fourier transform of the LDOS.

### IV. LOCAL DENSITY OF STATES

The LDOS can now be calculated directly from the Green function. In order to analyze the physical properties it is useful to consider the spatial Fourier transform of the LDOS as features like dispersing quasiparticles can be more easily identified. This technique was previously applied to the LDOS of Luttinger liquids<sup>6–8</sup> as well as CDW states and half-filled Mott insulators<sup>10,11</sup>. The Fourier transform of the LDOS for positive energies  $E > 0$  is given by<sup>30</sup>

$$N(E, Q) = -\frac{1}{2\pi} \int_{-\infty}^0 dx \int_{-\infty}^{\infty} dt e^{i(Et - Qx)} \times G_{\sigma\sigma}(\tau > 0, x, x) \Big|_{\tau \rightarrow it + \delta}. \quad (14)$$

Here the Green function has been analytically continued to real times and we have taken the limit  $x_1 \rightarrow x_2 \equiv x$ . We note that due to the assumed spin rotational invariance the LDOS does not depend on  $\sigma$ . As mentioned before, we will concentrate on the  $2k_F$ -component as it vanishes in the absence of the boundary and hence offers a particularly clean way of investigating boundary effects. For  $Q \approx 2k_F$  only  $G^{RL}$  contributes and starting

from (13) we arrive at our main result ( $|q| \ll 2k_F$ )

$$N(E, 2k_F + q) = -\Theta(E - 2\Delta) \sum_{k=0}^2 N_k(E, 2k_F + q), \quad (15)$$

$$N_k(E, 2k_F + q) = Z_2 \frac{e^{-i\pi/4} \sqrt{v_s}}{2\pi^{3/2}} \times \int \frac{d\theta_1 d\theta_2}{(2\pi)^2} \frac{\Theta(E - \Delta \sum_i \cosh \theta_i)}{\sqrt{E - \Delta \sum_i \cosh \theta_i}} \times \frac{h_k(\theta_1, \theta_2)}{v_s q_k - 2(E - \Delta \sum_i \cosh \theta_i) + i\delta}, \quad (16)$$

where

$$h_0(\theta_1, \theta_2) = \frac{1}{2} |G(\theta_1 - \theta_2)|^2,$$

$$h_1(\theta_1, \theta_2) = K(\theta_1 + i\frac{\pi}{2}) e^{\theta_1/4} G(\theta_2 - \theta_1) G(\theta_1 + \theta_2)^*,$$

$$h_2(\theta_1, \theta_2) = -\frac{1}{2} e^{(\theta_1 + \theta_2)/4} \prod_{i=1}^2 K(\theta_i + i\frac{\pi}{2}) \times \frac{\sinh \frac{\theta_1 + \theta_2 + i\pi}{\xi}}{\sinh \frac{\theta_1 + \theta_2}{\xi}} S_0(\theta_1 + \theta_2 + i\pi) |G(\theta_1 - \theta_2)|^2,$$

as well as  $q_0 = q$ ,  $q_1 = q - \frac{2\Delta}{v_c} \sinh \theta_1$ , and  $q_2 = q - \frac{2\Delta}{v_c} \sum_i \sinh \theta_i$ . Explicit integral representations for the scattering matrix  $S_0(\theta)$ , the boundary reflection matrix  $K(\theta)$ , and the function  $G(\theta)$  are given in App. B. Physically  $S_0(\theta)$  describes the scattering of two antisolitons with relative momentum corresponding to the rapidity  $\theta$ ,  $K(\theta)$  is the reflection amplitude of an antisoliton with rapidity  $\theta$  off the boundary [and thus incorporates the information on the boundary condition (7)], and  $G(\theta)$  appears in the matrix element [i.e. form factor] of the charge part of (8) and (9) with two-antisoliton states [see (A4)]. The parameter  $\xi$  is defined as  $\xi = \beta^2/(1 - \beta^2)$ . The normalization constant<sup>31</sup>  $Z_2$  has dimension  $Z_2 \propto \Delta^{\beta^2/16+1/\beta^2}$ ; thus in order to obtain dimensionless quantities we multiply the LDOS by  $\Delta^{3/2-\beta^2/16-1/\beta^2}/\sqrt{v_s}$  in all figures. The singularity of the integrands in (16) is smeared out by taking  $\delta$  small but finite; we choose  $\delta = 0.01$  unless stated otherwise. This mimics the broadening of singularities in experiments due to the instrumental resolution and the finite temperature. The LDOS (15) vanishes for  $E < 2\Delta$  as the fractionalization of an electron creates at least two antisolitons.

The three terms (16) constitute the leading contribution from the form-factor expansion. As can be seen from the double integrals they all originate in two-particle processes in the charge sector. The number of boundary reflection matrices  $K(\theta)$  indicates that  $N_k$  involves  $k$  interactions with the boundary, i.e. the terms (16) contain no, one, or two reflections of charge excitations. The sub-leading contributions involve at least three particles in the charge sector which either come from a higher number of particles in the intermediate state or from higher-order processes due to the boundary. Similar terms were

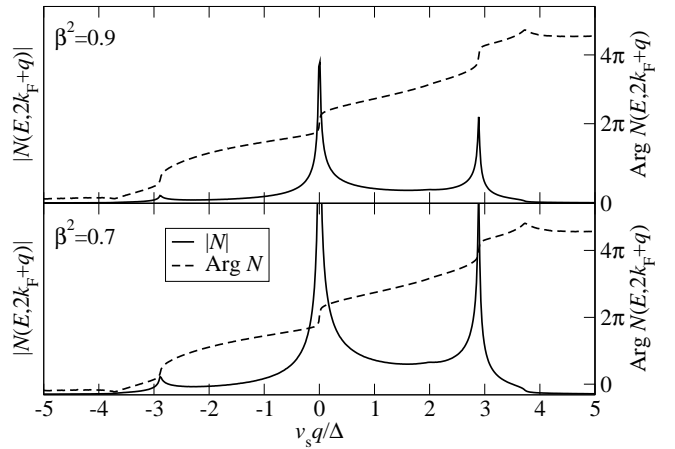


FIG. 1: Constant energy scan for  $E = 3\Delta$ :  $|N(E, 2k_F + q)|$  and  $\text{Arg } N(E, 2k_F + q)$  for  $v_c = 1.2 v_s$  and  $\beta^2 = 0.9$  (upper panel) and  $\beta^2 = 0.7$  (lower panel). Both plots are shown on the same scale. We observe a peak at  $q = 0$  and dispersing features at  $q = \pm 2\sqrt{(E - \Delta)^2 - \Delta^2}/v_c$  as well as  $q = \pm 2\sqrt{E^2 - 4\Delta^2}/v_c$ . For  $q < 0$  the dispersing features are strongly suppressed.

thoroughly analyzed for the LDOS in a CDW state at the LEP<sup>11</sup> as well as the spectral function in the Ising model with a boundary magnetic field<sup>32</sup>; they were found to be negligible in both cases. We further note that the suppression of sub-leading terms in the form-factor expansion for bulk two-point functions is a well-known feature of massive integrable field theories<sup>22,33</sup>. We thus expect the higher-order corrections to (15) to be negligible in the low-energy regime we consider here.

The constant energy scan of the Fourier transform of the LDOS (15) is shown in Fig. 1. We observe a singularity at  $q = 0$ , i.e.  $Q = 2k_F$ , which is indicative of the pinning of the  $2k_F$ -SDW at the boundary (see Sec. IV A). Furthermore there is a peak at  $q > 0$ . The constant momentum scans shown in Fig. 2 reveal that this peak shows dispersing behavior and splits above a critical momentum  $q > q_0$  [ $q_0$  will be defined in Eq. (22)]. More precisely these features follow the dispersion relations (19) and (20) respectively (see Sec. IV B). The existence of dispersing features is at first surprising since the spectral function<sup>17</sup> of the translationally invariant system does not show any dispersing quasiparticles. The processes contributing to the LDOS (15) can be thought of as arising from creating an electron at a position  $x$ , the fractionalization of this electron into at least one spinon and two antisolitons, the propagation of these elementary excitations through the system, and their subsequent recombination at the position  $x$ . This allows a natural interpretation of the leading terms in the form-factor expansion (16) in terms of propagating antisolitons and spinons. In the next sub-sections we will analyze the different terms (16) separately. Afterwards we comment on the different findings in the spectral function and the LDOS.

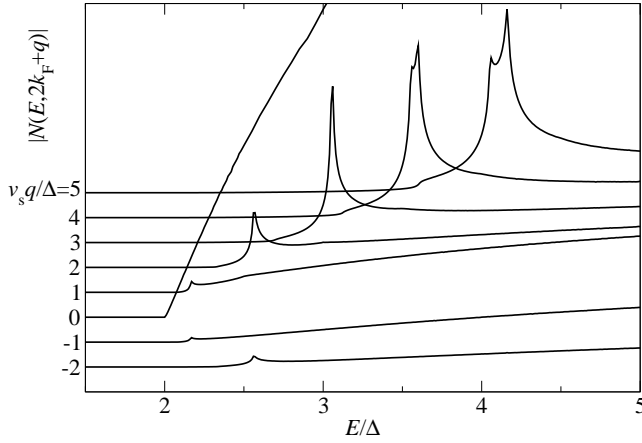


FIG. 2:  $|N(E, 2k_F + q)|$  for  $\beta^2 = 0.9$  and  $v_c = 1.2 v_s$ . The curves are constant  $q$ -scans which have been offset along the  $y$ -axis by a constant with respect to one another. The LDOS is dominated by the peak at  $q = 0$ . We further observe dispersing features at  $E_{1c} = \Delta + \sqrt{\Delta^2 + (v_c q/2)^2}$  as well as  $E_{1cs} = \Delta + \Delta \sqrt{1 - (v_s/v_c)^2} + v_s q/2$  for  $q > q_0$ .

#### A. No reflections in the charge sector: $N_0(E, 2k_F + q)$

Let us start with the analysis of the first term in the form-factor expansion (15), which is shown in Fig. 3. We first note that this term is dominated by a singularity at  $q = 0$ , i.e.  $Q = 2k_F$ . This singularity is due to the pinning of the  $2k_F$ -SDW at the boundary. As  $k_F = \pi/4a_0$  we find a spatial modulation with periodicity  $2\pi/2k_F = 4a_0$  as sketched<sup>13,34</sup> in Fig. 3.b. Close to  $q = 0$  the first term in the form-factor expansion and thus the whole LDOS behaves as<sup>35</sup>

$$N(E, 2k_F + q) \sim N_0(E, 2k_F + q) \sim \frac{1}{\sqrt{v_s q}}. \quad (17)$$

We note that the exponent is independent of the Luttinger parameter  $\beta$  (see Fig. 3.a). This singularity is similar to the ones observed in the LDOS of Luttinger liquids<sup>6,8</sup> as well as CDW states<sup>10,11</sup> where, however, the exponents depend on the interaction strength and thus the Luttinger parameter.

Furthermore,  $N_0$  possesses a weak dispersing feature following (see<sup>36</sup> Fig. 3.c)

$$E_s(q) = 2\Delta + \frac{v_s q}{2}, \quad q > 0. \quad (18)$$

As already discussed, the created electron fractionalizes into two antisolitons and (at least) one spinon which can propagate through the system. In this way of thinking the dispersing feature at  $E_s$  arises from two antisolitons with zero momentum (solid lines in Fig. 3.d) contributing an energy  $2\Delta$  and a massless soliton with momentum  $q$  (dashed line in Fig. 3.d). The appearance of  $v_s/2$  in  $E_s$  is due to the fact that the spinon has to propagate to the boundary and back, thus covering the distance  $2x$  in time  $t$ .

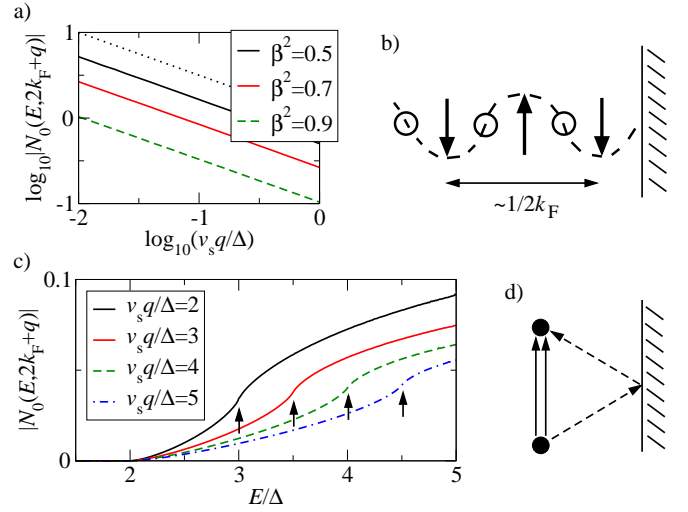


FIG. 3: (Color online)  $N_0(E, 2k_F + q)$  for  $v_c = 1.6 v_s$ . a) Logarithmic plot close to the singularity at  $q = 0$  for  $\delta = 0.001$ . The dotted line is a guide to the eye; it has gradient  $-1/2$ . b) Sketch<sup>13,34</sup> of the  $2k_F$ -SDW pinned at the boundary. c)  $|N_0(E, 2k_F + q)|$  for  $\beta^2 = 0.9$  and different momenta. We observe a dispersing feature at  $E_s = 2\Delta + v_s q/2$  indicated by small arrows. d) Sketch of the process giving rise to the propagating feature. The electron decomposes into two zero-momentum antisolitons (solid lines) and one spinon (dashed line) reflected at the boundary.

#### B. One reflection in the charge sector: $N_1(E, 2k_F + q)$

The next term in the form-factor expansion (15) contains one boundary reflection matrix  $K(\theta)$ . Thus it is natural to interpret it as arising from processes involving the reflection of one antisoliton at the boundary. In Fig. 4.a we show  $N_1$  for different momenta. We clearly observe a dispersing feature (indicated by up-arrows) following

$$E_{1c}(q) = \Delta + \sqrt{\Delta^2 + \left(\frac{v_c q}{2}\right)^2}. \quad (19)$$

This feature originates in the process where one anti-soliton propagates with momentum  $q$  while the other anti-soliton and the spinon possess zero momentum (see Fig. 4.b). The first term in  $E_{1c}$  is the rest mass of the zero-momentum anti-soliton while the second term is the energy of the propagating anti-soliton.

Furthermore, when  $q$  exceeds the critical value  $q_0$  a second dispersing feature appears (indicated by down-arrows in Fig. 4.a) at

$$E_{1cs}(q) = \Delta + \Delta \sqrt{1 - \left(\frac{v_s}{v_c}\right)^2} + \frac{v_s q}{2}. \quad (20)$$

The critical momentum  $q_0$  can be determined from the condition that the spin and charge excitations have the

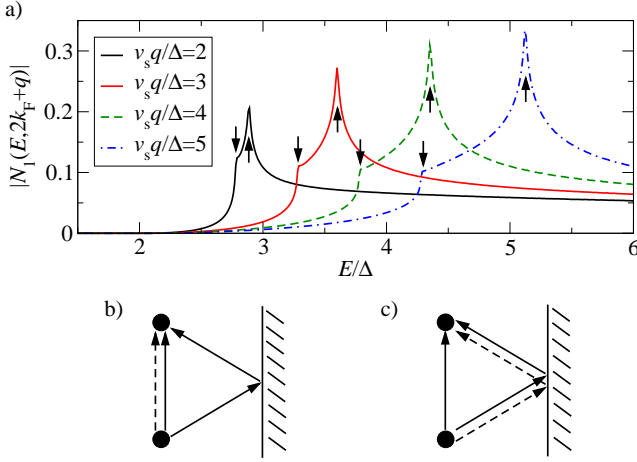


FIG. 4: (Color online) a)  $|N_1(E, 2k_F + q)|$  for  $\beta^2 = 0.9$ ,  $v_c = 1.6 v_s$ , and different momenta. We observe dispersing features at  $E_{1c} = \Delta + \sqrt{\Delta^2 + (v_c q/2)^2}$  indicated by up-arrows and  $E_{1cs} = \Delta + \Delta \sqrt{1 - (v_s/v_c)^2} + v_s q/2$  indicated by down-arrows. b) Process resulting in  $E_{1c}$ . The electron decomposes into one antisoliton and spinon with zero momentum as well as one antisoliton reflected at the boundary. c) Process resulting in  $E_{1cs}$ .

same group velocity

$$\left. \frac{\partial E_{1c}}{\partial q} \right|_{q=q_0} \stackrel{!}{=} \frac{\partial E_s}{\partial q} = \frac{v_s}{2}, \quad (21)$$

which leads to

$$q_0 = \frac{2\Delta v_s}{v_c \sqrt{v_c^2 - v_s^2}}. \quad (22)$$

Thus this feature can be thought of as arising from an antisoliton with momentum  $q_0$  and a spinon carrying momentum  $q - q_0$ , while the second antisoliton stays at rest (see Fig. 4.c). The fact that the propagating antisoliton and the spinon have the same group velocity results in an increased probability that both simultaneously arrive at position  $x$  after reflection at the boundary.

The observed splitting of the quasiparticle peak is reminiscent of what is found for the single-particle spectral function in the translationally invariant, half-filled Mott insulator<sup>37</sup> as well as the LDOS of a CDW state in the presence of a boundary in the regime of attractive interactions<sup>10,11</sup>. The peak splitting is a consequence of the curvature of the antisoliton dispersion (and thus of the charge gap) together with the condition  $v_c > v_s$ . Hence it cannot be observed in the Luttinger liquid case<sup>6-8</sup> where both sectors are massless.

### C. Two reflections in the charge sector: $N_2(E, 2k_F + q)$

The leading term in second order in the boundary reflection matrix is  $N_2$ . As in the previous term we find

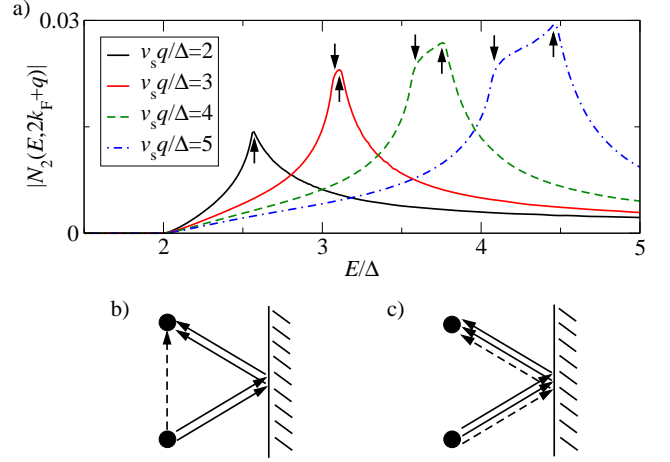


FIG. 5: (Color online) a)  $|N_2(E, 2k_F + q)|$  for  $\beta^2 = 0.9$ ,  $v_c = 1.6 v_s$ , and different momenta. We observe dispersing features at  $E_{2c} = 2\sqrt{\Delta^2 + (v_c q/4)^2}$  (up-arrows) and  $E_{2cs} = 2\Delta \sqrt{1 - (v_s/v_c)^2} + v_s q/2$  (down-arrows). Processes resulting in (b)  $E_{2c}$  and in (c)  $E_{2cs}$ .

two dispersing features. First, indicated by up-arrows in Fig. 5.a, there is a feature following

$$E_{2c}(q) = 2\sqrt{\Delta^2 + \left(\frac{v_c q}{4}\right)^2}. \quad (23)$$

This feature can be thought of as arising from the propagation of both antisolitons with momenta  $q/2$  and thus the same velocity, while the spinon has zero momentum (see Fig. 5.b). The second feature is found at

$$E_{2cs}(q) = 2\Delta \sqrt{1 - \left(\frac{v_s}{v_c}\right)^2} + \frac{v_s q}{2}, \quad (24)$$

provided  $q$  exceeds the critical momentum  $2q_0$ . This feature is indicated by down-arrows in Fig. 5.a. The interpretation is that both antisolitons carry momentum  $q_0$  while the excess momentum  $q - 2q_0$  is carried by the spinon (see Fig. 5.c).

We note that at finite momentum  $q > 0$  the term  $N_1$  dominates the LDOS as can be seen by comparing the scales in Figs. 3.c, 4.a, and 5.a, respectively. More importantly, the dispersing features originating in  $N_1$  are much more pronounced than those resulting from  $N_0$  and  $N_2$ . We attribute this to the fact that, at least in the naive interpretation of Figs. 4.b and c, the antisolitons involved in processes contributing to  $N_1$  possess different momenta as one of them is at rest while the other propagates through the system. In contrast, the dispersing features in  $N_0$  and  $N_2$  originate from processes in which the two antisolitons possess equal momenta (see Figs. 3.d as well as 5.b and c, respectively). Thus their relative rapidity vanishes and the scattering matrix is  $S_0(\theta = 0) = -1$  (see App. B). The resulting “quasi-fermionic” behavior leads to a strong suppression of the dispersing features in  $N_0$  and  $N_2$  via the Pauli principle.

Finally let us comment on the different findings in the spectral function<sup>17</sup> of the translationally invariant system and the LDOS (15) in the presence of a boundary. The spectral function is obtained from the Green function  $G(\tau, x, 0)$  via Fourier transformation with respect to  $t = -i\tau$  and  $x$ . The contributing processes require the propagation of all excitations, and in particular both antisolitons, from  $(0, 0)$  to  $(t, x)$ . Thus one may expect a dispersing feature at  $E = 2\sqrt{\Delta^2 + (v_c q/2)^2}$  from the antisolitons propagating with the same momentum  $q/2$ . In addition, above the critical momentum  $2q_0 = 2\Delta v_s/v_c \sqrt{v_c^2 - v_s^2}$  a linearly dispersing feature following  $E = 2\Delta \sqrt{1 - (v_s/v_c)^2} + v_s q$  is expected. Indeed these are exactly the conditions<sup>17</sup> for the threshold below which the spectral function vanishes. Above the threshold the spectral function is rather featureless, in particular there are no dispersing peaks associated with the propagation of charge or spin degrees of freedom. The absence of dispersing features may be attributed to the “quasi-fermionic” behavior of antisolitons, as all processes contributing to the spectral function will contain antisolitons with equal momenta. In contrast, the processes contributing to the LDOS (14) are given by the fractionalization of an electron at position  $x$ , the propagation of the two antisolitons and the spinon through the system, and the subsequent recombination at the original position  $x$ . In particular, processes where the momentum  $q$  is solely carried by one of the antisolitons or a spinon-antisoliton pair will contribute, resulting in the dispersing features at  $E_{1c}$  and  $E_{1cs}$ , respectively. The observation of these features thus underlines that the spectral function and the LDOS probe rather different physical processes. While the spectral function requires the propagation of all excitations between two points in the system, the LDOS also probes processes where only one or two excitations propagate to the impurity and back.

## V. LOCAL DENSITY OF STATES IN THE PRESENCE OF BOUNDARY BOUND STATES

Up to now we have concentrated on the boundary conditions (3) for the electron field or equivalently (7) for the canonical Bose fields. In this section we will consider more general phase shifts for the electron fields which lead to arbitrary Dirichlet boundary conditions for the Bose fields. As is well known, such boundary conditions can result in the existence of boundary bound states (BBS's), which are expected<sup>10,11</sup> to manifest themselves in the LDOS as features within the spectral gap. Here we will focus on general Dirichlet boundary conditions in the charge sector

$$\Phi_c(x=0) = \Phi_c^0, \quad -\frac{\pi}{\beta} \leq \Phi_c^0 \leq \frac{\pi}{\beta}, \quad (25)$$

while in the spin sector we still assume  $\Phi_s(x=0) = 0$ . In the boundary state formalism<sup>25</sup> applied here the information about the boundary condition (25) is encoded in

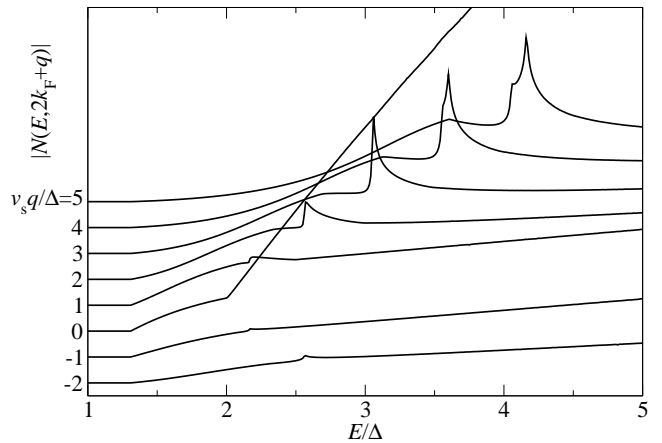


FIG. 6:  $|N(E, 2k_F + q)|$  for  $\beta^2 = 0.5$ ,  $\Phi_c^0 = -4$ , and  $v_c = 1.2 v_s$ . The curves are constant  $q$ -scans which have been offset along the y-axis by a constant with respect to one another. The existence of a BBS results in spectral weight within the two-soliton gap  $E < 2\Delta$ .

the boundary reflection matrix  $K(\theta)$ . In particular, the existence of a BBS will show up as a pole in the physical strip  $0 \leq \text{Im } \theta \leq \pi/2$ . As was shown in Ref. 38 this will be the case provided

$$-\frac{\pi}{\beta} < \Phi_c^0 < -\beta\pi; \quad (26)$$

the pole at  $\theta = i\gamma$  corresponds to a BBS with energy

$$E_{\text{bbs}} = \Delta \sin \gamma, \quad \gamma = \frac{\pi + \beta\Phi_c^0}{2 - 2\beta^2}. \quad (27)$$

When calculating the Green function the pole of the boundary reflection matrix will lead to two additional terms,  $\mathcal{G}_3$  and  $\mathcal{G}_4$ , in the form-factor expansion (13). This in turn yields two additional terms in the LDOS (15).

To be explicit, let us consider the LEP  $\beta^2 = 1/2$  in the following. The three leading terms in the form-factor expansion of the LDOS are still given by (16) where the boundary reflection matrix now depends explicitly on  $\Phi_s^0$

$$K(\theta) = \frac{\sin(i\frac{\theta}{2} - \frac{\Phi_c^0}{\sqrt{8}})}{\cos(i\frac{\theta}{2} + \frac{\Phi_c^0}{\sqrt{8}})}. \quad (28)$$

This obviously possesses a pole in the physical strip  $0 \leq \text{Im } \theta \leq \pi/2$  provided  $\Phi_c^0 < -\pi/\sqrt{2}$  corresponding to the existence of a BBS. The resulting two additional terms in the LDOS read ( $k = 3, 4$ )

$$\begin{aligned} N_k(E, 2k_F + q) &= Z_2 \sqrt{v_s} \cos \frac{\Phi_c^0}{\sqrt{2}} \frac{e^{-i(\pi - \sqrt{2}\Phi_c^0)/8}}{\pi^{3/2}} \\ &\times \int \frac{d\theta}{2\pi} \frac{\Theta(E - \Delta \cosh \theta - E_{\text{bbs}})}{\sqrt{E - \Delta \cosh \theta - E_{\text{bbs}}}} \\ &\times \frac{h_k(\theta)}{v_s q_k - 2(E - \Delta \cosh \theta - E_{\text{bbs}}) + i v_s \kappa_{\text{bbs}}}, \quad (29) \end{aligned}$$

where

$$h_3(\theta) = \left| \sinh \frac{\theta + \frac{1}{2}(\pi + \sqrt{2}\Phi_c^0)}{2} \right|^2,$$

$$h_4(\theta) = -K(\theta + i\frac{\pi}{2}) e^{\theta/4} \sinh^2 \frac{\theta - \frac{1}{2}(\pi + \sqrt{2}\Phi_c^0)}{2},$$

$$E_{\text{bbs}} = -\Delta \sin \frac{\Phi_c^0}{\sqrt{2}}, \quad \kappa_{\text{bbs}} = -\frac{2\Delta}{v_c} \cos \frac{\Phi_c^0}{\sqrt{2}},$$

as well as  $q_3 = q$  and  $q_4 = q - \frac{2\Delta}{v_c} \sinh \theta$ . We note that  $\kappa_{\text{bbs}} > 0$  has the dimension of an inverse length. The spatial dependence of the terms  $\mathcal{G}_3$  and  $\mathcal{G}_4$  (see App. A) is dominated by  $\sim e^{\kappa_{\text{bbs}}x}$  ( $x < 0$ ), thus it is natural to interpret  $1/\kappa_{\text{bbs}}$  as the width of the BBS.

The terms (29) possess a threshold at  $E = \Delta + E_{\text{bbs}}$  corresponding to the creation of the boundary bound state and an additional antisoliton. Interestingly, although  $N_3$  and  $N_4$  separately possess jumps at the threshold, the sum of both terms is continuous. This is reminiscent of the BBS contributions in the Ising model with a boundary magnetic field<sup>32</sup>, where a cancellation of singularities yields a smooth spectral function at the threshold.

The LDOS in the presence of a BBS is shown in Fig. 6. We clearly observe a contribution within the gap  $E < 2\Delta$ . In contrast to BBS's in the CDW state<sup>10,11</sup> there is, however, no singularity at  $E = E_{\text{bbs}}$  as the underlying processes involve the creation of a spinon, an antisoliton, and the BBS. As before the LDOS is dominated by a singularity at  $q = 0$  and we observe dispersing features following (19) and (20) respectively.

## VI. COMPARISON TO HALF-FILLED MOTT INSULATOR

The LDOS of a half-filled Mott insulator in the presence of a boundary was analyzed in detail<sup>39</sup> in Ref. 11. As already mentioned, the effective low-energy Hamiltonian is also given by (4)–(6) but the expressions for the right- and left-moving Fermi fields in terms of the Bose fields differ from (8) and (9). From the physical point of view right- and left-moving Fermi fields create and annihilate individual antisolitons in the half-filled case whereas they create and annihilate antisoliton pairs in the quarter-filled system. Thus the gap in the LDOS is given by  $\Delta$  in the former and  $2\Delta$  in the latter system. Apart from this we find the following similarities and differences.

In both cases the LDOS possesses a singularity at  $q = 0$  which behaves as  $N(E, 2k_F + q) \sim 1/\sqrt{v_s q}$  independently<sup>40</sup> of the Luttinger parameter  $\beta$ . This singularity is due to the pinning of the  $2k_F$ -SDW at the boundary, which possesses a wave length  $2a_0$  or  $4a_0$  respectively.

Beside this singularity the LDOS of the half-filled Mott insulator shows dispersing features at  $E = \sqrt{\Delta^2 + (v_c q/2)^2}$ , at  $E = \Delta + v_s q/2$ , and, for  $q > q_0$ , at  $E = \Delta\sqrt{1 - (v_s/v_c)^2} + v_s q/2$ . An interpretation is

obtained by noting that the electron decomposes into one spinon and one antisoliton, which then propagate through the system. As the leading processes involve only individual antisolitons, the "quasi-fermionic" behavior of the antisolitons discussed at the end of Sec. IV C does not affect the LDOS. In contrast, in the quarter-filled system we observe only two dispersing modes following (19) and (20) respectively (see Fig. 2). All other dispersing features discussed above are strongly suppressed due to the "quasi-fermionic" behavior of the antisolitons.

Finally, in the presence of a BBS with energy  $E_{\text{bbs}} < \Delta$  the LDOS of the half-filled Mott insulator possesses a non-dispersing singularity with  $N(E, 2k_F + q) \sim 1/\sqrt{E - E_{\text{bbs}}}$  which originates from the creation of a spinon and the BBS. In contrast, in the quarter-filled case the LDOS is smooth at the threshold  $E = \Delta + E_{\text{bbs}}$  which originates from the simultaneous creation of one antisoliton and the BBS.

## VII. DISCUSSION AND EXPERIMENTAL SIGNATURES

In this section we compare qualitative aspects of the LDOS of various one-dimensional systems in the presence of a boundary or strong impurity potential. We discuss the spatial Fourier transform  $N(E, Q)$  defined in (14). Specifically we consider Luttinger liquids<sup>6</sup>, half-filled Mott insulators (or CDW states)<sup>10,11</sup>, and the quarter-filled Mott insulator investigated in Sec. IV. We focus on the  $Q \approx 2k_F$ -component of the LDOS as it vanishes in the translationally invariant systems and thus provides a particularly clean way to investigate boundary effects. (We note that the LDOS in the small-momentum regime  $Q \approx 0$  behaves qualitatively similar.) The first feature, which all three systems have in common, is a singularity of the LDOS  $N(E, 2k_F + q)$  at  $q = 0$ , which originates in the pinning of a charge or spin density wave at the impurity. In the case of a Luttinger liquid the strength of this singularity depends on the Luttinger parameter  $K_c$  and thus on the interactions between the electrons, whereas in both the half-filled and quarter-filled Mott insulator the LDOS behaves as<sup>40</sup>  $N(E, 2k_F + q) \sim 1/\sqrt{q}$ . Furthermore, as was pointed out in Ref. 22, the gap of the LDOS in the half-filled Mott insulator is given by the soliton mass  $\Delta$ , which equals the thermal activation gap and is half of the gap observed in optical measurements. In contrast, in the quarter-filled system the LDOS possesses a gap of  $2\Delta$ , which is equal to the optical gap but twice the thermal gap.

In addition, the LDOS possesses various dispersing features (see Fig. 7). In the Luttinger liquid case one observes two linearly dispersing modes corresponding to individually propagating spin and charge degrees of freedom respectively (see Fig. 7.a). In the half-filled Mott insulator an electron decomposes into massless spin excitations and one charge excitation with mass  $\Delta$ . Propagating spin excitations give rise to a linearly dispersing mode



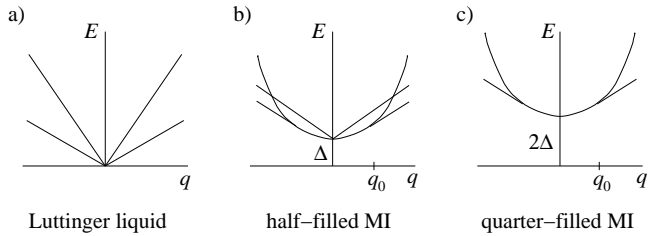


FIG. 7: Schematic picture of the dispersing features observable in the spatial Fourier transform  $N(E, 2k_F + q)$  of the LDOS in different one-dimensional systems. a) In a Luttinger liquid one finds two linearly dispersing modes. b) In a half-filled Mott insulator (MI) there exists a gap  $\Delta$ . One observes one linear and one curved dispersion. From the latter a third feature splits off at  $q = q_0$ . c) The quarter-filled Mott insulator possesses a gap  $2\Delta$ . One further observes one curved dispersion from which a linear mode splits off at  $q = q_0$ . In both (b) and (c) the thermal activation gap is given by  $\Delta$ .

with velocity  $v_s$ , while the propagating charge excitation results in a curved dispersion relation. In addition, there exists a critical momentum  $q = q_0$  at which the group velocity of the charge excitation equals  $v_s$ . At this momentum a third linearly dispersing feature splits away from the charge mode, which has its origin in the collective propagation of spin and charge degrees of freedom with equal velocities (see Fig. 7.b). We note that the qualitative behavior discussed for the half-filled Mott insulator is also expected in other systems possessing gapless excitations in one sector and gapped ones in the other like, for instance, CDW states. Finally, in the quarter-filled Mott insulator an electron decomposes into massless spin excitations and two charge excitations with masses  $\Delta$ . This results in a curved dispersion originating in the propagation of one charge excitation while the second one stays at the position of the STM tip. This dispersion splits at the critical momentum  $q_0$  due to the collective propagation of one charge excitation and additional spin degrees of freedom (see Fig. 7.c). We note that one does not observe individually propagating spin excitations. The relevant processes would require the two charge excitations to possess equal momenta, which is forbidden by their "quasi-fermionic" behavior (see Sec. IV C).

To sum up, at sufficiently large momenta  $q$  we observe two linearly dispersing modes in a Luttinger liquid, two linear and one curved dispersion relation in a half-filled Mott insulator, and one linear and one curved dispersion in a quarter-filled Mott insulator. This clearly demonstrates that characteristic properties of the bulk state of matter and its electronic excitations can be inferred from studying spatial modulations of the LDOS in the presence of an impurity.

The LDOS discussed in this article is directly related to the tunneling current measured in STM experiments. If the density of states in the STM tip is approximately independent of energy, the tunneling conductance will be given by the thermally smeared LDOS of the sample at

the position of the tip<sup>1</sup>

$$\frac{dI(V, x)}{dV} \propto \int dE f'(E - eV) N(E, x), \quad (30)$$

where  $f(E)$  denotes the Fermi function.  $N(E, Q)$  can then easily be obtained via spatial Fourier transformation. In this context the models discussed above apply to quasi-one-dimensional materials at energies above the cross-over scale to three-dimensional behavior. This situation might be experimentally realized for example in stripe phases of high-temperature superconductors<sup>1,6</sup>, carbon nanotubes<sup>3,41</sup>, Bechgaard and Fabre salts<sup>16</sup>, self-organized atomic gold chains<sup>42</sup>, and two-leg ladder materials<sup>43</sup>.

As discussed above already the knowledge of qualitative properties such as the presence of a spectral gap and its relation to the thermal activation gap as well as the number and positions of singularities can reveal substantial information about the electronic properties and excitations of quasi-one-dimensional materials. A more detailed analysis of quantitative features like the strength of singularities or the precise positions of dispersing modes can even lead to estimates for the Luttinger parameter and the velocities of charge and spin excitations. There are, of course, experimental limitations. Obviously the experimental resolution and thermal broadenings have to be sufficiently small to clearly distinguish the different singularities and dispersing modes. Moreover, the simplified relation (30) does not contain<sup>1</sup> the matrix elements for the tunneling from the sample into the tip, which may introduce a non-trivial spatial dependence of the tunneling conductance on the LDOS and thus hamper a natural interpretation in terms of propagating excitations.

## VIII. CONCLUSIONS

In conclusion, we have studied a quarter-filled Mott insulator in the presence of an impurity, which was modeled by a boundary condition for the electron fields. In this system we calculated the  $2k_F$ -component of the spatial Fourier transform of the LDOS using the boundary state formalism together with a form-factor expansion. The LDOS is dominated by a singularity at  $Q = 2k_F$ , which is indicative of a pinning of a SDW at the impurity. Furthermore, we observed several dispersing features above the two-soliton gap  $E < 2\Delta$ . We identified their physical origin as spin and charge degrees of freedom, which propagate between the STM tip and the impurity, and attributed their relative strength to the "quasi-fermionic" behavior of charge excitations with equal momenta. This also explains the absence of dispersing features in the spectral function<sup>17</sup> of the translationally invariant system and underlines that the spectral function and the LDOS probe rather different physical processes. We further showed that a BBS in the charge sector leads to

a non-vanishing LDOS within the two-soliton gap. Finally, we discussed our results in the context of other one-dimensional systems, i.e. Luttinger liquids and half-filled Mott insulators, and argued that the measurement of the spatial modulations in the LDOS can be used to extract detailed informations about the electronic states of quasi-one-dimensional systems.

### Acknowledgments

I would like to thank Fabian Essler, Markus Garst, Markus Morgenstern, Alexei Tsvelik, and particularly Volker Meden for valuable discussions and comments. This work was supported by the German Research Foundation (DFG) through the Emmy Noether Program.

### Appendix A: Calculation of the Green function

In this appendix we derive the leading terms  $\mathcal{G}_k$  in the form-factor expansion of the charge part of the Green function (13), i.e. we determine the correlation function

$$\langle O_R(\tau, x_1) O_L^\dagger(0, x_2) \rangle \quad (\text{A1})$$

$$C_{n2m}(\tau, x_1, x_2) = \frac{1}{2^m} \frac{1}{m!} \frac{1}{n!} \int_{-\infty}^{\infty} \frac{d\theta'_1 \dots d\theta'_m}{(2\pi)^m} \int_{-\infty}^{\infty} \frac{d\theta_1 \dots d\theta_n}{(2\pi)^n} K^{a_1 b_1}(\theta'_1) \dots K^{a_m b_m}(\theta'_m) \times \langle 0 | O_R(\tau, x_1) | \theta_n, \dots, \theta_1 \rangle_{c_n, \dots, c_1}^{c_1, \dots, c_n} \langle \theta_1, \dots, \theta_n | O_L^\dagger(0, x_2) | -\theta'_1, \theta'_1, \dots, -\theta'_m, \theta'_m \rangle_{a_1, b_1, \dots, a_m, b_m}. \quad (\text{A3})$$

Here the states  $|\theta_n, \dots, \theta_1\rangle_{c_n, \dots, c_1}$  (and so on) are scattering states of solitons and antisolitons, the indices  $a_i, b_i, c_i$  take the values  $\mp 1$  and label the corresponding U(1) charges, and energy and momentum of solitons and antisolitons are given in terms of the rapidities  $\theta_i$  and  $\theta'_i$  by (10). We note that (A2) constitutes an expansion in two parameters: (i) the number of particles (with rapidities  $\theta_i$ ) in the intermediate state and (ii) the number of reflections of particles at the boundary [the number of boundary reflection matrices  $K(\theta'_i)$ ].

The scattering of solitons or antisolitons with rapidities  $\theta_1$  and  $\theta_2$  is encoded in the scattering matrix<sup>44</sup>  $|\theta_1, \theta_2\rangle_{ab} = S_{ab}^{cd}(\theta_1 - \theta_2) |\theta_2, \theta_1\rangle_{dc}$ . The boundary reflection matrix<sup>25</sup>  $K^{ab}(\theta)$  similarly describes the reflection at the boundary,  $|\theta\rangle_a = K^{\bar{a}b}(i\frac{\pi}{2} - \theta) |-\theta\rangle_b$ , where  $\bar{a} = \pm$  for  $a = \mp$ . For Dirichlet boundary conditions one has<sup>25,38</sup>  $K^{++}(\theta) = K^{--}(\theta) = 0$ .

Furthermore,  $O(\tau, x) = e^{-xH} e^{-iP\tau} O e^{iP\tau} e^{xH}$ , where  $H$  and  $P$  are the Hamiltonian and the total momentum of the sine-Gordon model on the infinite line. The operator  $O_R$  ( $O_L^\dagger$ ) creates (annihilates) two antisolitons, i.e. increases (decreases) the U(1) charge by 2. The necessary

in the sine-Gordon model (5) on the half line. Here the operators  $O_R^\dagger$  and  $O_L^\dagger$  are given by the charge parts of (8) and (9) respectively. We calculate (A1) using the boundary state formalism<sup>25</sup> together with a form-factor expansion<sup>22,28,29</sup>. The same technique was previously applied<sup>10,11</sup> to determine the Green function of a CDW state in the presence of an impurity. Here we restrict ourselves to the main steps of the derivation and concentrate on the differences as compared to Ref. 11, to which we refer implicitly for all details and definitions not discussed here.

By performing a rotation in Euclidean space we map<sup>25</sup> the problem onto the sine-Gordon model on the real axis. The boundary condition is translated into an initial condition encoded in a boundary state. Expanding the latter in powers of the boundary reflection matrix and inserting a resolution of the identity between the operators in (A1) we find

$$\langle O_R(\tau, x_1) O_L^\dagger(0, x_2) \rangle = \sum_{n=0}^{\infty} \sum_{m=0}^{\infty} C_{n2m}(\tau, x_1, x_2), \quad (\text{A2})$$

where we have defined the auxiliary functions

form factors were derived by Lukyanov and Zamolodchikov<sup>31</sup>. In our conventions they are given by

$$\langle 0 | O_{R/L} | \theta_1, \theta_2 \rangle_{--} = \sqrt{Z_2} e^{\pm i\pi/8} e^{\pm(\theta_1 + \theta_2)/8} G(\theta_1 - \theta_2), \quad (\text{A4})$$

where the normalization constant  $Z_2$  and the auxiliary function  $G(\theta)$  are stated in App. B. The form factors satisfy the form-factor axioms as stated in Ref. 11 with Lorentz spin  $s(O_{R/L}) = \pm 1/4$  and semi-locality factor  $l_-(O_{R/L}) = e^{\pm i\pi/4}$ . In the following we will evaluate the terms  $C_{20}$ ,  $C_{22}$ , and  $C_{24}$  which result in  $\mathcal{G}_0$ ,  $\mathcal{G}_1$ , and  $\mathcal{G}_2$ , respectively.

#### 1. Derivation of $\mathcal{G}_0$

The first term to be evaluated is  $C_{20}$ . It does not contain any information about the boundary in the charge sector, i.e. it contains no boundary reflection matrices. A similar term was calculated in Ref. 17 in the derivation of the spectral function in the translationally invari-

ant system. After shifting the contour of integration,  $\theta_{1,2} \rightarrow \theta_{1,2} + i\pi/2$ , we directly obtain

$$\mathcal{G}_0 = C_{20} = \frac{Z_2}{2} e^{i\pi/4} \int_{-\infty}^{\infty} \frac{d\theta_1 d\theta_2}{(2\pi)^2} |G(\theta_1 - \theta_2)|^2 \times e^{i\frac{\Delta}{v_c} r \sum_i \sinh \theta_i} e^{-\Delta \tau \sum_i \cosh \theta_i},$$

where the center-of-mass coordinates are defined by  $x = (x_1 + x_2)/2 < 0$  and  $r = x_1 - x_2 < 0$ . Analytical continuation  $\tau \rightarrow it$  to real times, taking the limit  $r \rightarrow 0$ , and Fourier transformation (14) with respect to  $t$  and  $x$  yield the first term  $N_0(E, 2k_F + q)$  in the form-factor expansion of the LDOS (15).

## 2. Derivation of $\mathcal{G}_1$

We start with  $C_{22}$  defined in (A3). As the operator  $O_R$  creates two antisolitons we deduce  $c_1 = c_2 = -$ ;  $K^{++}(\theta') = K^{--}(\theta') = 0$  yields  $b = \bar{a}$ . The matrix element of  $O_L^\dagger$  contains incoming and outgoing particles and thus possesses kinematical poles. We deal with these terms following Smirnov<sup>28</sup> and analytically continue the form factor as (see Ref. 11 for a detailed discussion of this procedure)

$$\begin{aligned} & -- \langle \theta_1, \theta_2 | O_L^\dagger | -\theta', \theta' \rangle_{a\bar{a}} \\ &= -- \langle \theta_1 + i0, \theta_2 + i0 | O_L^\dagger | -\theta', \theta' \rangle_{a\bar{a}} \\ & \quad + 2\pi \delta(\theta_1 - \theta') \delta_{-\bar{a}} - \langle \theta_2 | O_L^\dagger | -\theta' \rangle_a \quad (A5) \\ & \quad + 2\pi \delta(\theta_1 + \theta') \delta_{-b} S_{a\bar{a}}^{bc}(-2\theta') - \langle \theta_2 | O_L^\dagger | \theta' \rangle_c \\ & \quad + 2\pi \delta(\theta_2 - \theta') \delta_{e\bar{a}} S_{--}^{de}(\theta_1 - \theta_2)^d \langle \theta_1 | O_L^\dagger | -\theta' \rangle_a \\ & \quad + 2\pi \delta(\theta_2 + \theta') \delta_{be} S_{a\bar{a}}^{bc}(-2\theta') \\ & \quad \times S_{--}^{de}(\theta_1 - \theta_2)^d \langle \theta_1 | O_L^\dagger | \theta' \rangle_c. \end{aligned}$$

Here we have already omitted the positive imaginary parts of the rapidities in the form factors in the 2nd to 5th lines as they do not possess kinematical poles. Inserting (A5) into  $C_{22}$  yields to different contributions: The first line leads to a term containing three integrations over rapidities and is thus a sub-leading correction; we will not evaluate it here. The 2nd to 5th lines yield using the boundary cross-unitarity condition<sup>25</sup>  $K^{ab}(\theta) = S_{cd}^{ab}(2\theta) K^{dc}(-\theta)$  as well as unitarity<sup>44</sup>  $S_{a_1 a_2}^{c_1 c_2}(\theta) S_{c_1 c_2}^{b_1 b_2}(-\theta) = \delta_{a_1}^{b_1} \delta_{a_2}^{b_2}$

$$\begin{aligned} & \int_{-\infty}^{\infty} \frac{d\theta'}{2\pi} \frac{d\theta}{2\pi} K^{+-}(\theta') \langle 0 | O_R | \theta, \theta' \rangle_{--} - \langle \theta | O_L^\dagger | -\theta' \rangle_+ \\ & \quad \times e^{i\Delta \tau (\sinh \theta + \sinh \theta')} e^{\frac{\Delta}{v_c} (r \cosh \theta + 2x \cosh \theta')}. \quad (A6) \end{aligned}$$

In order to proceed let us first assume  $\Phi_c^0 = 0$ . This implies that the boundary reflection matrix does not depend on the U(1) charge, i.e.  $K^{+-}(\theta') = K^{-+}(\theta') = K(\theta')$ , where  $K(\theta)$  is explicitly stated in App. B. In particular,  $K(\theta')$  is analytic in the physical strip  $0 \leq \text{Im} \theta' \leq \pi/2$ .

Now we shift the contours of integration  $\theta, \theta' \rightarrow \theta, \theta' + i\pi/2$  (we note that the contribution originating in the first term of (A5) does not possess any poles in the physical strip  $0 \leq \text{Im} \theta_i \leq \pi/2$ ) and apply the crossing relation in the second form factor,

$$\begin{aligned} & - \langle \theta + i\frac{\pi}{2} | O_L^\dagger | -\theta' - i\frac{\pi}{2} \rangle_+ = + \langle -\theta' + i\frac{\pi}{2} | O_L | \theta - i\frac{\pi}{2} \rangle_-^* \\ & = e^{-i\pi/4} \langle 0 | O_L | -\theta' + i\frac{3\pi}{2}, \theta - i\frac{\pi}{2} \rangle_{--}^*, \end{aligned}$$

where the phase factor  $e^{-i\pi/4}$  is due to the semi-locality<sup>22,28,29</sup> of the operator  $O_L$  with respect to the fundamental fields creating the excitations. Finally we use (A4) to obtain

$$\begin{aligned} \mathcal{G}_1 &= Z_2 e^{i\pi/4} \int_{-\infty}^{\infty} \frac{d\theta'}{2\pi} \frac{d\theta}{2\pi} K(\theta' + i\frac{\pi}{2}) G(\theta - \theta') G(\theta + \theta')^* \\ & \quad \times e^{\theta'/4} e^{i\frac{\Delta}{v_c} (r \sinh \theta + 2x \sinh \theta')} e^{-\Delta \tau (\cosh \theta + \cosh \theta')}. \end{aligned}$$

Fourier transformation (14) directly yields the second term  $N_1(E, 2k_F + q)$  of the LDOS.

On the other hand, if  $\Phi_c^0 < -\beta\pi$ , the boundary reflection matrix  $K^{+-}(\theta')$  possesses a pole at  $\theta' = i\gamma$ . At the LEP the residue is given by  $2i \cos(\Phi_c^0/\sqrt{2})$  (see (28)). Thus when shifting the contours of integration in (A6) we obtain the additional BBS contribution

$$\begin{aligned} \mathcal{G}_3 &= -2i Z_2 \cos \frac{\Phi_c^0}{\sqrt{2}} e^{-i(\pi - \sqrt{2}\Phi_c^0)/8} e^{-E_{\text{BBS}}\tau} e^{\kappa_{\text{BBS}}x} \\ & \quad \times \int_{-\infty}^{\infty} \frac{d\theta}{2\pi} \left| \sinh \frac{\theta + i\frac{1}{2}(\pi + \sqrt{2}\Phi_c^0)}{2} \right|^2 e^{i\frac{\Delta}{v_c} r \sinh \theta} e^{-\Delta \tau \cosh \theta}. \end{aligned}$$

Fourier transformation yields  $N_3(E, 2k_F + q)$ .

## 3. Derivation of $\mathcal{G}_2$

Finally we calculate the leading term involving the reflection of two antisolitons, which originates from  $C_{24}$ . The analytic continuation of the form factor of  $O_L^\dagger$  reads

$$\begin{aligned} & -- \langle \theta_1, \theta_2 | O_L^\dagger | -\theta'_1, \theta'_1, -\theta'_2, \theta'_2 \rangle_{a\bar{a}\bar{b}\bar{b}} \\ &= -- \langle \theta_1 + i0, \theta_2 + i0 | O_L^\dagger | -\theta'_1, \theta'_1, -\theta'_2, \theta'_2 \rangle_{a\bar{a}\bar{b}\bar{b}} \\ & \quad + S_{-+}^{-+}(\theta'_1 + \theta'_2) \delta_{+a} \delta_{+b} \quad (A7) \\ & \quad \times -- \langle \theta_1, \theta_2 | \theta'_1, \theta'_2 \rangle_{--} \langle 0 | O_L^\dagger | -\theta'_1, -\theta'_2 \rangle_{++} \\ & \quad + S_{a\bar{a}}^{-+}(-2\theta'_1) S_{-+}^{-+}(-\theta'_1 + \theta'_2) \delta_{+b} \\ & \quad \times -- \langle \theta_1, \theta_2 | -\theta'_1, \theta'_2 \rangle_{--} \langle 0 | O_L^\dagger | \theta'_1, -\theta'_2 \rangle_{++} \\ & \quad + S_{b\bar{b}}^{-+}(-2\theta'_2) S_{-+}^{-+}(\theta'_1 - \theta'_2) \delta_{+a} \\ & \quad \times -- \langle \theta_1, \theta_2 | \theta'_1, -\theta'_2 \rangle_{--} \langle 0 | O_L^\dagger | -\theta'_1, \theta'_2 \rangle_{++} \\ & \quad + S_{a\bar{a}}^{-+}(-2\theta'_1) S_{b\bar{b}}^{-+}(-2\theta'_2) S_{-+}^{-+}(-\theta'_1 - \theta'_2) \\ & \quad \times -- \langle \theta_1, \theta_2 | -\theta'_1, -\theta'_2 \rangle_{--} \langle 0 | O_L^\dagger | \theta'_1, \theta'_2 \rangle_{++}, \end{aligned}$$

where the scalar products are evaluated using the Faddeev-Zamolodchikov algebra<sup>44,45</sup>

$$\begin{aligned} & -- \langle \theta_1, \theta_2 | \theta'_1, \theta'_2 \rangle_{--} = (2\pi)^2 [\delta(\theta_1 - \theta'_2) \delta(\theta_2 - \theta'_1) \\ & \quad + S_{--}(\theta'_1 - \theta_2) \delta(\theta_1 - \theta'_1) \delta(\theta_2 - \theta'_2)]. \end{aligned}$$

Therefore the 2nd to 5th line in (A7) yield (we also use the scattering axiom for the first form factor)

$$\begin{aligned} & \frac{1}{2} \int_{-\infty}^{\infty} \frac{d\theta'_1 d\theta'_2}{(2\pi)^2} K^{+-}(\theta'_1) K^{+-}(\theta'_2) S_{-+}^{-+}(\theta'_1 + \theta'_2) \\ & \times \langle 0 | O_R | \theta'_1, \theta'_2 \rangle_{--} \langle 0 | O_L^\dagger | -\theta'_1, -\theta'_2 \rangle_{++} \\ & \times e^{i\Delta\tau \sum_i \sinh \theta'_i} e^{2\frac{\Delta}{v_c} x \sum_i \cosh \theta'_i}. \end{aligned} \quad (\text{A8})$$

Let us again first assume  $\Phi_c^0 = 0$ . If we shift the contours of integration  $\theta'_i \rightarrow \theta'_i + i\pi/2$  and use the crossing relation as well as a Lorentz transformation,

$$\begin{aligned} & \langle 0 | O_L^\dagger | -\theta'_1 - i\frac{\pi}{2}, -\theta'_2 - i\frac{\pi}{2} \rangle_{++} \\ & = e^{-i\pi/8} \langle 0 | O_L | -\theta'_2, -\theta'_1 \rangle_{--}^*, \end{aligned}$$

we obtain

$$\begin{aligned} \mathcal{G}_2 &= \frac{Z_2}{2} e^{i\pi/4} \int_{-\infty}^{\infty} \frac{d\theta'_1 d\theta'_2}{(2\pi)^2} K(\theta'_1 + i\frac{\pi}{2}) K(\theta'_2 + i\frac{\pi}{2}) \\ & \times S_{-+}^{-+}(\theta'_1 + \theta'_2 + i\pi) |G(\theta'_1 - \theta'_2)|^2 \\ & \times e^{(\theta'_1 + \theta'_2)/4} e^{2i\frac{\Delta}{v_c} x \sum_i \sinh \theta'_i} e^{-\Delta\tau \sum_i \cosh \theta'_i}. \end{aligned}$$

$N_2(E, 2k_F + q)$  is now readily obtained via Fourier transformation.

Starting from (A8) the second term  $N_4(E, 2k_F + q)$  related to the BBS is obtained by picking up the poles of  $K^{+-}(\theta'_1)$  and  $K^{+-}(\theta'_2)$  at  $\theta'_{1,2} = i\gamma$  respectively. At the LEP the result is

$$\begin{aligned} \mathcal{G}_4 &= 2i Z_2 \cos \frac{\Phi_c^0}{\sqrt{2}} e^{-i(\pi - \sqrt{2}\Phi_c^0)/8} e^{-E_{\text{bbs}}\tau} e^{\kappa_{\text{bbs}}x} \\ & \times \int_{-\infty}^{\infty} \frac{d\theta'}{2\pi} K^{+-}(\theta' + i\frac{\pi}{2}) \sinh^2 \frac{\theta' - \frac{1}{2}(\pi + \sqrt{2}\Phi_c^0)}{2} \\ & \times e^{\theta'/4} e^{i\frac{\Delta}{v_c} r \sinh \theta'} e^{-\Delta\tau \cosh \theta'}. \end{aligned}$$

## Appendix B: Explicit expressions for form factors and scattering matrices

In this appendix we collect some formulas on the sine-Gordon theory used in the present article. The scattering

matrix between solitons and antisolitons possesses the integral representation<sup>22</sup>

$$S_0(\theta) = -\exp \left[ i \int_0^\infty \frac{dt}{t} \sin \frac{\theta t}{\pi\xi} \frac{\sinh(\frac{t}{2}(1 - \frac{1}{\xi}))}{\sinh \frac{t}{2} \cosh \frac{t}{2\xi}} \right],$$

where  $\xi = \beta^2/(1 - \beta^2)$ . A similar integral representation for the boundary reflection matrix reads<sup>46</sup> (for Dirichlet boundary conditions with  $\Phi_c^0 = 0$ )

$$\begin{aligned} K(\theta) &= -\cos \left( \frac{\pi}{2\xi} + i\frac{\theta}{\xi} \right) R_0(i\frac{\pi}{2} - \theta) \sigma(i\frac{\pi}{2} - \theta), \\ R_0(\theta) &= \exp \left[ 2i \int_0^\infty \frac{dt}{t} \sin \frac{\theta t}{\pi\xi} \sinh \frac{3t}{4\xi} \frac{\sinh(\frac{t}{4}(1 - \frac{1}{\xi}))}{\sinh \frac{t}{4} \sinh \frac{t}{\xi}} \right], \\ \sigma(\theta) &= \exp \left[ 2i \int_0^\infty \frac{dt}{t} \sin \frac{\theta t}{\pi\xi} \frac{\sinh(\frac{t}{\xi}(1 + i\frac{\theta}{\pi}))}{\sinh t \cosh \frac{t}{\xi}} \right]. \end{aligned}$$

The auxiliary function  $G(\theta)$  appearing in the form factors (A4) is given by<sup>31</sup>

$$\begin{aligned} G(\theta) &= -i\mathcal{C}_1 \sinh \frac{\theta}{2} \\ & \times \exp \left[ \int_0^\infty \frac{dt}{t} \frac{\sinh^2(t(1 + i\frac{\theta}{\pi})) \sinh(t(\xi - 1))}{\sinh(2t) \cosh t \sinh(t\xi)} \right], \\ \mathcal{C}_1 &= \exp \left[ - \int_0^\infty \frac{dt}{t} \frac{\sinh^2 \frac{t}{2} \sinh(t(\xi - 1))}{\sinh(2t) \cosh t \sinh(t\xi)} \right], \end{aligned}$$

while for the normalization factor  $Z_2$  one finds numerically from the integral representation derived in Ref. 31

$$\begin{aligned} Z_2 &\approx 7.7320 \Delta^{1681/1440} \quad \text{for } \beta^2 = 0.9, \\ Z_2 &\approx 20.1857 \Delta^{1649/1120} \quad \text{for } \beta^2 = 0.7. \end{aligned}$$

The expressions at the LEP are obtained by setting  $\xi = 1$  ( $\beta^2 = 1/2$ ), i.e.  $S_0(\theta) = -1$ ,  $K(\theta) = i \tanh \frac{\theta}{2}$ ,  $G(\theta) = -i \sinh \frac{\theta}{2}$ , and  $Z_2 \approx 38.5519 \Delta^{65/32}$ .

<sup>1</sup> O. Fischer, M. Kugler, I. Maggio-Aprile, C. Berthod, and C. Renner, *Rev. Mod. Phys.* **79**, 353 (2007).

<sup>2</sup> J. E. Hoffman, K. McElroy, D.-H. Lee, K. M. Lang, H. Eisaki, S. Uchida, and J. C. Davis, *Science* **297**, 1148 (2002); K. McElroy, R. W. Simmonds, J. E. Hoffman, D.-H. Lee, J. Orenstein, H. Eisaki, S. Uchida, and J. C. Davis, *Nature* **422**, 592 (2003); C. Howald, H. Eisaki, N. Kaneko, M. Greven, and A. Kapitulnik, *Phys. Rev. B* **67**, 014533 (2003); M. Vershinin, S. Misra, S. Ono, Y. Abe, Y. Ando, and A. Yazdani, *Science* **303**, 1995 (2004).

<sup>3</sup> J. Lee, S. Eggert, H. Kim, S.-J. Kahng, H. Shinohara, and Y. Kuk, *Phys. Rev. Lett.* **93**, 166403 (2004).

<sup>4</sup> M. Fabrizio and A. O. Gogolin, *Phys. Rev. B* **51**, 17827 (1995); S. Eggert, H. Johannesson, and A. Mattsson, *Phys. Rev. Lett.* **76**, 1505 (1996); S. Eggert, *ibid.* **84**, 4413 (2000); M. Guigou, T. Martin, and A. Crépieux, *Phys. Rev. B* **80**, 045420 (2009).

<sup>5</sup> V. Meden, W. Metzner, U. Schollwöck, O. Schneider, T. Stauber, and K. Schönhammer, *Eur. Phys. J. B* **16**, 631 (2000).

<sup>6</sup> S. A. Kivelson, I. P. Bindloss, E. Fradkin, V. Oganesyan, J. M. Tranquada, A. Kapitulnik, and C. Howald, *Rev. Mod. Phys.* **75**, 1201 (2003).

<sup>7</sup> P. Kakashvili, H. Johannesson, and S. Eggert, *Phys. Rev. B*

- 74, 085114 (2006).
- <sup>8</sup> I. Schneider and S. Eggert, Phys. Rev. Lett. **104**, 036402 (2010).
  - <sup>9</sup> G. Bedürftig, B. Brendel, H. Frahm, and R. M. Noack, Phys. Rev. B **58**, 10225 (1998).
  - <sup>10</sup> D. Schuricht, F. H. L. Essler, A. Jaefari, and E. Fradkin, Phys. Rev. Lett. **101**, 086403 (2008).
  - <sup>11</sup> D. Schuricht, F. H. L. Essler, A. Jaefari, and E. Fradkin, Phys. Rev. B **83**, 035111 (2011).
  - <sup>12</sup> C. L. Kane and M. P. A. Fisher, Phys. Rev. Lett. **68**, 1220 (1992); Phys. Rev. B **46**, 15233 (1992); A. Furusaki and N. Nagaosa, Phys. Rev. B **47**, 4631 (1993).
  - <sup>13</sup> T. Giamarchi, *Quantum Physics in One Dimension* (Oxford University Press, Oxford, 2004).
  - <sup>14</sup> T. Giamarchi, Physica B **230-232**, 975 (1997); M. Nakamura, Phys. Rev. B **61**, 16377 (2000); H. Yoshioka, M. Tsuchiizu, and Y. Suzumura, J. Phys. Soc. Jpn. **69**, 651 (2000); **70**, 762 (2001).
  - <sup>15</sup> F. Mila and X. Zotos, Europhys. Lett. **24**, 133 (1993); K. Penc and F. Mila, Phys. Rev. B **49**, 9670 (1994); K. Sano and Y. Ōno, J. Phys. Soc. Jpn. **63**, 1250 (1994); Phys. Rev. B **70**, 155102 (2004); S. Ejima, F. Gebhard, and S. Nishimoto, Europhys. Lett. **70**, 492 (2005); K. Sano and Y. Ōno, Phys. Rev. B **75**, 113103 (2007).
  - <sup>16</sup> H. Seo, C. Hotta, and H. Fukuyama, Chem. Rev. **104**, 5005 (2004); T. Giamarchi, *ibid.* **104**, 5037 (2004); D. Jérôme, *ibid.* **104**, 5565 (2004).
  - <sup>17</sup> F. H. L. Essler and A. M. Tsvelik, Phys. Rev. Lett. **88**, 096403 (2002).
  - <sup>18</sup> F. Zwick, S. Brown, G. Margaritondo, C. Merlic, M. Onelion, J. Voit, and M. Grioni, Phys. Rev. Lett. **79**, 3982 (1997).
  - <sup>19</sup> D. Controzzi, F. H. L. Essler, and A. M. Tsvelik, Phys. Rev. Lett. **86**, 680 (2001); F. H. L. Essler, F. Gebhard, and E. Jeckelmann, Phys. Rev. B **64**, 125119 (2001); S. Andergassen, T. Enss, V. Meden, W. Metzner, U. Schollwöck, and K. Schönhammer, *ibid.* **73**, 045125 (2006); T. Shirakawa and E. Jeckelmann, *ibid.* **79**, 195121 (2009).
  - <sup>20</sup> Starting from (4.24) in Ref. 13 with  $n = 2$  we rescale the Bose fields according to  $\phi_\rho \rightarrow \beta\Phi_c/\sqrt{32}$  and  $\theta_\rho \rightarrow \Theta_c/\sqrt{2}\beta$  with  $\beta^2 = 4K$ . The double-Umklapp term is relevant for  $K < 1/4$ , i.e. for  $\beta < 1$ .
  - <sup>21</sup> A. Schwartz, M. Dressel, G. Grüner, V. Vescoli, L. Degiorgi, and T. Giamarchi, Phys. Rev. B **58**, 1261 (1998); M. Dressel, K. Petukhov, B. Salameh, P. Zornoza, and T. Giamarchi, *ibid.* **71**, 075104 (2005). B. Korin-Hamzić, E. Tafra, M. Basletić, A. Hamzić, and M. Dressel, *ibid.* **73**, 115102 (2006).
  - <sup>22</sup> F. H. L. Essler and R. M. Konik, in *From fields to strings: Circumnavigating theoretical physics (Ian Kogan Memorial Collection)*, edited by M. Shifman, A. Vainshtein, and J. Wheeler (World Scientific, Singapore, 2005), Vol. I.
  - <sup>23</sup> A. B. Zamolodchikov, Int. J. Mod. Phys. A **10**, 1125 (1995).
  - <sup>24</sup> A. Luther and V. J. Emery, Phys. Rev. Lett. **33**, 589 (1974).
  - <sup>25</sup> S. Ghoshal and A. B. Zamolodchikov, Int. J. Mod. Phys. A **9**, 3841 (1994); *ibid.* **9**, 4353(E) (1994).
  - <sup>26</sup> A. MacIntyre, J. Phys. A: Math. Gen. **28**, 1089 (1995); H. Saleur, S. Skorik, and N. P. Warner, Nucl. Phys. B **441**, 421 (1995).
  - <sup>27</sup> P. Di Francesco, P. Mathieu, and D. Sénéchal, *Conformal Field Theory* (Springer, New York, 1997).
  - <sup>28</sup> F. A. Smirnov, *Form factors in completely integrable models of quantum field theory* (World Scientific, Singapore, 1992).
  - <sup>29</sup> S. Lukyanov, Commun. Math. Phys. **167**, 183 (1995).
  - <sup>30</sup> The LDOS for  $E < 0$  can be analyzed in the same way.
  - <sup>31</sup> S. Lukyanov and A. B. Zamolodchikov, Nucl. Phys. B **607**, 437 (2001).
  - <sup>32</sup> D. Schuricht and F. H. L. Essler, J. Stat. Mech. P11004, 2007.
  - <sup>33</sup> J. L. Cardy and G. Mussardo, Nucl. Phys. B **410**, 451 (1993).
  - <sup>34</sup> H. Seo and H. Fukuyama, J. Phys. Soc. Jpn. **66**, 1249 (1997).
  - <sup>35</sup> The small momentum regime is dominated by a similar singularity,  $N(E, Q) \sim N_0(E, Q) \sim 1/Q$ .
  - <sup>36</sup> This feature is more pronounced in  $\text{Re } N_0(E, 2k_F + q)$ .
  - <sup>37</sup> J. Voit, Eur. Phys. J. B **5**, 505 (1998); F. H. L. Essler and A. M. Tsvelik, Phys. Rev. B **65**, 115117 (2002); F. H. L. Essler and A. M. Tsvelik, Phys. Rev. Lett. **90**, 126401 (2003); H. Benthien, F. Gebhard, and E. Jeckelmann, *ibid.* **92**, 256401 (2004); T. Ulbricht and P. Schmitteckert, Europhys. Lett. **89**, 47001 (2010).
  - <sup>38</sup> P. Mattsson and P. Dorey, J. Phys. A: Math. Gen. **33**, 9065 (2000).
  - <sup>39</sup> The half-filled Mott insulator is equivalent to the attractive regime of a CDW state discussed in Sec. IV.B of Ref. 11 with  $k_F = \pi/2a_0$  and  $K_c = 1$ .
  - <sup>40</sup> In contrast, in a CDW state the strength of this singularity depends<sup>11</sup> on the Luttinger parameter  $K_c$  in the gapless charge sector.
  - <sup>41</sup> T. W. Odom, J.-L. Huang, and C. M. Lieber, J. Phys.: Condens. Matter **14**, R145 (2002).
  - <sup>42</sup> J. Schäfer, C. Blumenstein, S. Meyer, M. Wisniewski, and R. Claessen, Phys. Rev. Lett. **101**, 236802 (2008); P. C. Snijders and H. H. Weitering, Rev. Mod. Phys. **82**, 307 (2010).
  - <sup>43</sup> P. Abbamonte, G. Blumberg, A. Rusydi, A. Gozar, P. G. Evans, T. Siegrist, L. Venema, H. Eisaki, E. D. Isaacs, and G. A. Sawatzky, Nature **431**, 1078 (2004); S. Notbohm, P. Ribeiro, B. Lake, D. A. Tennant, K. P. Schmidt, G. S. Uhrig, C. Hess, R. Klingeler, G. Behr, B. Büchner, M. Reehuis, R. I. Bewley, C. D. Frost, P. Manuel, and R. S. Eccleston, Phys. Rev. Lett. **98**, 027403 (2007).
  - <sup>44</sup> A. B. Zamolodchikov and Al. B. Zamolodchikov, Ann. Phys. **120**, 253 (1979).
  - <sup>45</sup> L. D. Faddeev, Sov. Sci. Rev. Math. Phys. C **1**, 107 (1980).
  - <sup>46</sup> J.-S. Caux, H. Saleur, and F. Siano, Nucl. Phys. B **672**, 411 (2003).